

Complete Clinicopathological Case Report of a Young Patient Dying of COVID-19–Related Stroke

Laura D. Taylor, MBChB, DipForMed(SA)Path, MMed Path (Foren), FCForPath (SA),*
Ozayr Saleh Ameen, MBChB, FCNeurol, † and Stefan-Dan Zaharie, MBChB, EFN‡

Abstract: The SARS-CoV-2 (severe acute respiratory syndrome coronavirus 2) pandemic has revealed diverse neurological manifestations of coronavirus disease 2019 (COVID-19). This case report begins with a background review of the neurological effects of COVID-19, focusing on stroke, neuroinflammation, and coagulopathy. It then describes the clinical course and autopsy findings of a young patient presenting with COVID-19–associated stroke. The formal neuropathological examination is presented, along with the systemic and brain histological features. Interesting aspects include multiterritory hemorrhagic infarctions, microinfarcts throughout the cortex and white matter, and prominent mixed inflammatory cell cuffing of intracerebral blood vessels distant from the infarcts.

Key Words: COVID-19, histopathological correlation, neuropathology, stroke

(*Am J Forensic Med Pathol* 2021;42: 160–163)

The severe acute respiratory syndrome coronavirus 2 (SARS-CoV-2) pandemic has revealed diverse potential neurological complications of coronavirus disease 2019 (COVID-19). Coronaviruses are established neurovirulent organisms, and neurological symptoms occur in 88% of patients with severe disease.¹ Hematogenous spread to the brain may occur through damaged capillary endothelium or by binding angiotensin-converting enzyme 2 (ACE2) receptors to cross the blood-brain barrier, where virus enters neurons and glial cells.^{1–4} Dissemination via retrograde transport in the olfactory bulb is another possibility. Once in the brain, transsynaptic transfer has been postulated.⁵

One major complication of “neuro-COVID” is stroke, which may be linked to SARS-CoV-2 hypercoagulability.

COVID-19 patients have a stroke incidence 8 times higher than those hospitalized with influenza, occurring in 3% of hospitalized patients, with an incidence of 6% in those with severe disease. Stroke may be the first presentation of COVID-19 but is usually delayed with respect to symptom onset.^{6,7} In a series from China, predominantly older COVID-19 stroke patients with other cardiovascular risk factors were described, with an incidence of 5% among hospitalized patients.⁸ On the other hand, young patients with COVID-19 and large-vessel stroke are rarely described. A recent report documented 5 cases of large-vessel stroke in

patients younger than 50 years in whom COVID-19 infection was diagnosed.⁹

The independent relationship of viral respiratory tract infection and ischemic stroke is not a new concept.² General viral infections increase stroke risk due to vascular inflammation, platelet activation, and hypercoagulability. Additionally, inflammatory destabilization of atheromatous plaques is a suggested mechanism.^{2,4} Influenza viruses aggravate ischemic brain injury as well as increase the risk of hemorrhage after thrombolytic therapy.⁶ Large-vessel stroke has also been previously reported in association with SARS-CoV-1.¹⁰ It should be observed that secondary infarcts may be due to the general hypotension and hypoxia in patients with severe systemic illness.⁶

There are many possible mechanisms of stroke; however, as yet, there is no proven direct causal link.² Comorbidities common to both COVID-19 and stroke, such as diabetes, obesity, and hypertension, may partly explain the coincidence of the 2 pathologies. Such patients are often older, with more evidence of systemic inflammation.^{4,5} These factors strongly influence microglial phenotype, which modulates the local effect of the virus in the brain.⁴ Of interest, ACE2 receptor expression is increased in ischemic brains and in the brains of diabetics, making viral entry to the CNS more likely.³ In turn, viral binding to ACE2 receptors can raise blood pressures, increasing the risk of cerebral hemorrhage.⁶

Extensive thrombosis in capillaries and small vessels of the venous and arterial systems is a well-established feature of severe COVID-19.² Local thrombosis can be purely the result of disseminated intravascular coagulation, and secondary thromboemboli may occur.³ Direct virally mediated endothelial cell injury also predisposes to thrombosis and has been demonstrated in postmortem histology of various systemic organs, excluding the brain.¹¹ Other potential causes of cerebral vasculitis are immune-mediated damage and viral invasion of inflammatory cells themselves. This is also postulated to account for polymerase chain reaction (PCR)–negative meningoencephalitis.⁶ In addition to thrombosis, cerebral vasculitis may lead to direct hemorrhage.⁴

In the few reported cases without other cardiovascular risk factors, SARS-CoV-2–induced hypercoagulability is the mostly likely mechanism.⁵ SARS-CoV-2 is an RNA virus, and extracellular RNA serves as a template for contact-dependent thrombosis, activating proteases including factors XI and XII.¹² As a neurotropic virus, SARS-CoV-2 could activate glial cells, resulting in a proinflammatory state.⁶ However, the “cytokine storm” associated with severe COVID-19 occurs even without direct CNS invasion. Proinflammatory cytokines activate endothelial and mononuclear cells, with increased tissue factor expression. This initiates coagulation, generates thrombin, and activates platelets, leading to thrombosis. The highly prothrombotic state is clinically reflected by elevated D-dimer, ferritin, and interleukin 6 levels.¹¹ Interleukin 6 is produced in the lungs, as well as by infected neurons.¹¹ Concentrations are negatively correlated with T-cell numbers and predict symptom severity, outcome, and stroke risk.^{4,6} It has also been suggested that COVID-19 may stimulate

Manuscript received October 5, 2020; accepted November 17, 2020.

From the *Division of Forensic Medicine and Toxicology, University of Cape Town Faculty of Health Sciences; †Melomed Gatesville Medical Centre; and ‡Division of Anatomical Pathology, Tygerberg Hospital, Cape Town, South Africa.

The authors declare no conflict of interest.

Reprints: Laura D. Taylor, MBChB, DipForMed(SA)Path, MMed Path (Foren), FCForPath (SA), Division of Forensic Medicine and Toxicology, University of Cape Town Faculty of Health Sciences, Anzio Road, Observatory, 7705, Cape Town, South Africa. E-mail: Laura.Taylor@uct.ac.za.

Approval for the publication of this case report was received from the University of Cape Town Human Research Ethics Committee (study no. HREC 541/2020). Informed consent was also signed by the deceased's next of kin.

Copyright © 2021 Wolters Kluwer Health, Inc. All rights reserved.

ISSN: 0195-7910/21/4202-0160

DOI: 10.1097/PAF.0000000000000668

TABLE 1. Selected Laboratory Results From Terminal Admission*

Procalcitonin	0.567 (0.0–0.500) ng/mL
White blood cell count	16 (4–11) × 10 ⁹ /L
C-reactive protein	278 (<5) mg/L
Ferritin	1179.3 (15–150) µg/L
Interleukin 6	287 (<7) pg/mL
Platelet count	411 (140–420) × 10 ⁹ /L
Hemoglobin A _{1c}	6.8% (3.9%–6.1%)

*Reference ranges in parentheses.

antiphospholipid antibody production, although the pathogenic relevance of this remains uncertain.⁷

CASE REPORT

Clinical Course

The deceased was a 40-year-old woman with no known comorbidities who was admitted with pneumonia and diagnosed with SARS-CoV-2 by polymerase chain reaction. A further respiratory viral panel and blood culture were negative. She received intravenous methylprednisolone 40 mg daily and enoxaparin 80 mg twice daily, as well as vitamin C and zinc orally. She was discharged after 5 days but re-presented 2 days later, 2 hours after sudden collapse. Selected blood results from this admission are presented in Table 1. On examination, she had dense right-sided weakness (Medical Research Council score 0/5 in the right upper and right lower limbs), aphasia, a right gaze palsy, right hemianopia, and right hemisensory loss. Her National Institutes of Health Stroke Score was 24.

An urgent computed tomography (CT) brain scan showed a complete occlusion of the M1 branch of the left middle cerebral artery (MCA) with features of early ischemia. Her Alberta Stroke Program Early CT score was 6. Because she presented within the critical time window and there were no contraindications, intravenous thrombolysis (alteplase 72 mg) was given. She was then sent for mechanical thrombectomy. Pump aspiration resulted in patency of the M1 segment; however, the angular branch remained occluded. After this procedure, she was extubated. The following morning, she managed to speak and eat but remained densely paralyzed on the right side. Unfortunately, 21 hours after stroke onset, her level of consciousness dropped, requiring intubation and ventilation. A repeat CT brain scan showed massive ischemic infarction in the left MCA territory with a parenchymal hematoma (hemorrhagic transformation). There was significant swelling resulting in entrapment hydrocephalus, subfalcine, and uncal herniation. The CT findings were in keeping with malignant infarction of the left hemisphere. Cryoprecipitate and fresh frozen plasma were immediately infused when this postlysis bleed was diagnosed. Subsequently, the left pupil became fixed and dilated, and an urgent decompressive left hemicraniectomy was performed. Despite this, there was no clinical improvement, and the patient developed hemodynamic instability and arrested approximately 48 hours after brainstem death.

Autopsy

This case was referred to Forensic Pathology Services for investigation of a procedure-related death, in terms of South African law.¹ The autopsy was performed using locally published infection-control procedures, using full personal protective equipment.²

¹Inquests Act 58 of 1959, Health Professions Act 56 of 1974 (as amended).

²Standard Operating Procedure guidelines available on request

The examination was undertaken after a postmortem interval of 6 days; however, there were no macroscopic features of decomposition.

The decedent was overweight, with a body mass index of 27 kg/m². Medical additions, including the craniectomy wound, were noted. Examination of the lungs showed numerous subpleural petechial hemorrhages. Both lungs were posteriorly congested and edematous, with no consolidation. The heart was of normal weight with no left ventricular hypertrophy and only minimal circumferential nonocclusive atherosclerosis present in the coronary arteries. There was no patent foramen ovale or septal defect. The common, internal, and external carotid arteries were free of thrombus, and there were no visible plaques or fatty streaks. The liver appeared mildly fatty. The renal surfaces were smooth, with no finely granular appearance suggestive of systemic hypertension.

A 12-mL clotted extradural hemorrhage was found on opening the skull. The brain mushroomed anteriorly and medially out of the craniectomy defect in the left frontal and parietal bones. The fresh brain weighed 1496 g. It was fixed in formalin for formal neuropathological examination, and fragments of olfactory bulb were placed into glutaraldehyde for electron microscopy.

Systemic Histology

All systemic organs were sampled. There were fibrin thrombi, confirmed with Martius scarlet blue stains, in the capillaries, arterioles, and venules of the lungs, kidney, liver, and pancreas. There was a large amount of hemosiderin in the spleen, possibly relating to red blood cell damage from intravascular fibrin. Glycogenated hepatocyte nuclei were noted, representing chronically raised blood sugar levels. Of interest given her recent admission for pneumonia, the lungs demonstrated pulmonary edema, scattered interstitial lymphocytes, and intra-alveolar macrophages with mild patchy parenchymal fibrosis. There was no evidence of active diffuse alveolar damage.

Neuropathological Findings

Externally, the cerebral hemispheres were swollen with left-to-right midline shift. The left frontoparietal cerebral mushroom demonstrated hemorrhagic softening of the herniated tissue. There was a left frontal burst lobe with a small amount of subdural hemorrhage. The superior sagittal sinus was free of thrombus and the circle of Willis and its branches were similarly unremarkable, being macroscopically free of atherosclerotic plaque. Coronal sections confirmed hemorrhagic infarction of the left MCA and anterior cerebral artery (ACA) territories, in keeping with multiterritory arterial occlusion or a venous infarct.

Tissue sections were taken for histology. There were multifocal fibrin thrombi, including in sites distant from the infarcts. Blood vessels were globally congested. Several of the small blood vessels throughout the brain demonstrated cuffing by mononuclear inflammatory cells and neutrophils, particularly in the brainstem where there was also a focal increase in lymphocytes in the meninges. CD45 immunohistochemistry highlighted these perivascular and intravascular monocytes. The left ACA and MCA sections demonstrated large hemorrhagic infarcts with a neutrophilic response, highlighted by a myeloperoxidase stain. Red neurons and axonal spheroids were identified, indicating hypoxic-ischemic injury. Gitter cells and CD68⁺ tissue macrophages were present in the penumbra. Cortex and white matter distant from the arterial territory infarcts also demonstrated microinfarcts with spongiosis/necrosis and red neurons. Axonal varicosities and spheroids were highlighted with a neurofilament protein stain. There was perivascular extravasation of red blood cells in these areas. Laminar cortical necrosis was noted; however, this finding may

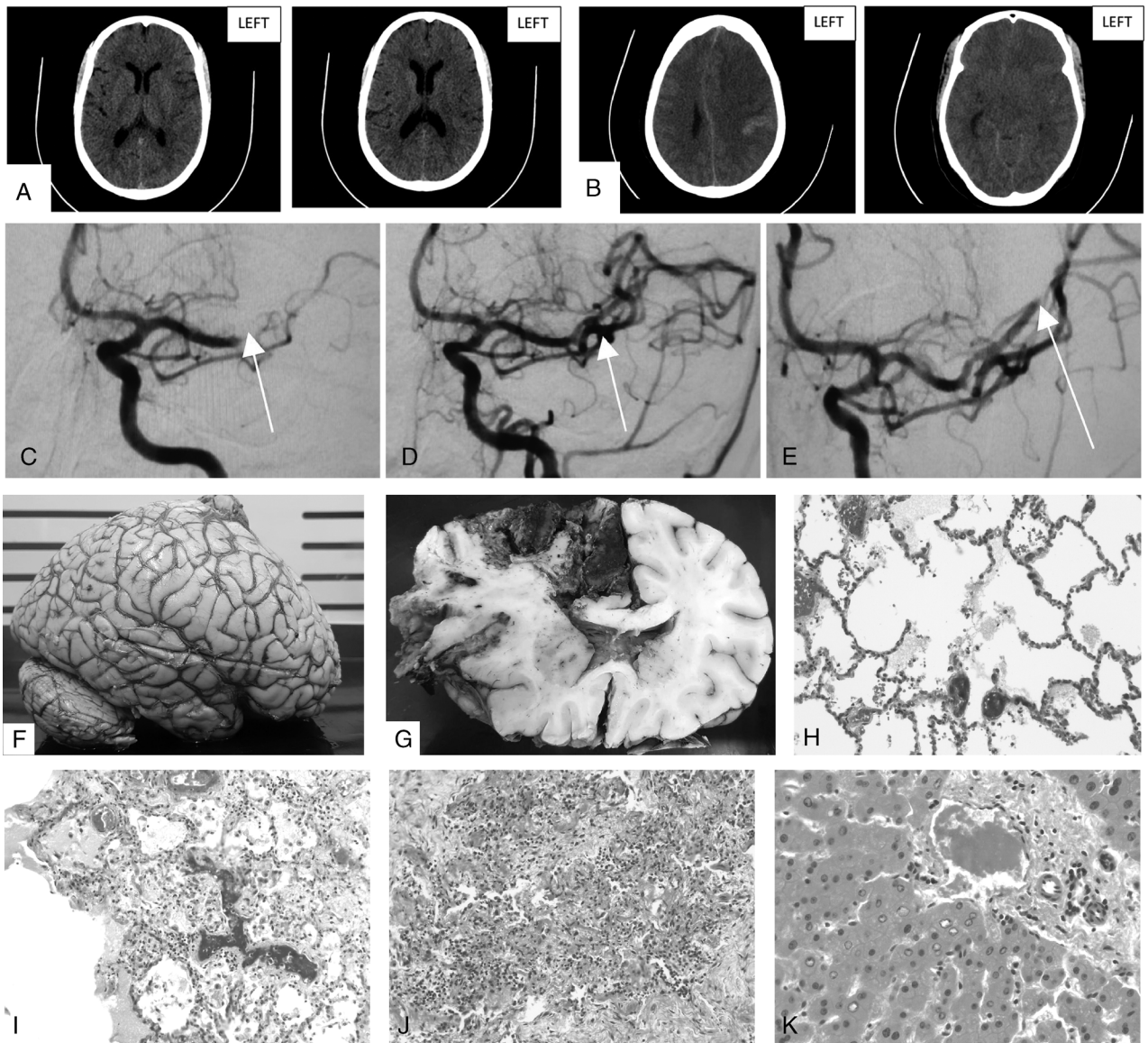


FIGURE 1. A, Initial precontrast CT brain scan showing loss of definition of the lateral left lentiform nucleus and insular ribbon with mild sulcal effacement and loss of gray-white matter differentiation in the high MCA territory. B, Follow-up uncontrasted CT brain scan showing malignant left hemisphere infarction with small parenchymal hemorrhage and associated mass effect. C, Initial angiogram of left MCA with arrow indicating site of occlusion. D, Angiogram post-pump aspiration of left MCA with arrow showing restoration of flow. E, Angiogram of the left MCA showing persistent occlusion of the angular branch. F, External surface of fixed brain demonstrating swelling. G, Coronal section of fixed brain with left AMA and MCA territory hemorrhagic infarction and left-to-right midline shift. H, Pulmonary blood vessels with fibrin thrombi (hematoxylin-eosin stain, original magnification $\times 200$). I, Lung parenchyma with intravascular fibrin thrombi, scattered interstitial lymphocytes, and intra-alveolar macrophages (hematoxylin-eosin stain, original magnification $\times 100$). J, Focal pulmonary fibrosis with scattered lymphocytes (hematoxylin-eosin stain, original magnification $\times 100$). K, Hepatic portal tract with fibrin thrombus in the venule and adjacent glycogenated hepatocyte nuclei (hematoxylin-eosin stain, original magnification $\times 400$). L, Spleen demonstrating hemosiderin deposition (Perls Prussian blue stain, original magnification $\times 100$). M, Left ACA territory infarct with intravascular fibrin thrombus (Martius scarlet blue stain, original magnification $\times 200$). N, Left ACA territory infarct with fibrin thrombus in blood vessel, surrounded by mixed inflammatory cells and associated spongiosis (hematoxylin-eosin stain, original magnification $\times 400$). O, Left MCA territory hemorrhagic infarct demonstrating red neurons, neutrophils, and macrophages (hematoxylin-eosin stain, original magnification $\times 200$). P, Left MCA territory infarct with red neurons (hematoxylin-eosin stain, original magnification $\times 400$). Q, Pontine microinfarct with axonal spheroids and spongiosis (hematoxylin-eosin stain, original magnification $\times 400$). R, Pontine microinfarct with red neurons and spongiosis (hematoxylin-eosin stain, original magnification $\times 200$). S, Pontine blood vessel fibrin thrombus (hematoxylin-eosin stain, original magnification $\times 200$). T, Right MCA microinfarct with spongiosis, axonal spheroids, and perivascular inflammatory cells (hematoxylin-eosin stain, original magnification $\times 200$). U, Right ACA territory blood vessel at leptomeninges with surrounding mixed inflammatory cells (hematoxylin-eosin stain, original magnification $\times 400$; [I, J] hematoxylin-eosin stain, original magnification $\times 100$; [H, O, R, S, T] hematoxylin-eosin stain, original magnification $\times 200$; [K, N, P, Q, U] hematoxylin-eosin stain, original magnification $\times 400$; [L] Perls Prussian blue stain, original magnification $\times 100$; [M] Martius scarlet blue stain, original magnification $\times 200$).

be related to poor perfusion during the period of brain death. Electron microscopy performed on a sample of olfactory nerve was noncontributory because of autolysis (Fig. 1).

DISCUSSION

Clinical-neuropathological correlation is key to establishing the extent of COVID-19 involvement in humans.³ In a recent series, retrospective chart analysis from COVID-19 patients who died within 32 days of symptom onset showed that all these patients exhibited confusion or delayed arousal. Histology of their brains showed evidence of hypoxia, but not encephalitis or other virus-specific changes. Immunohistochemical viral staining was negative, although RNA was detected at low levels.¹³

Inflammatory changes appear to be variable. Our patient had meningeal involvement, and isolated meningoencephalitis has been clinically reported, occurring with or without detection of SARS-Cov-2 in the cerebrospinal fluid by polymerase chain reaction.^{5,14} Other histological contributions show a spectrum of pathology, from isolated brainstem perivascular lymphocyte accumulations to necrotizing hemorrhagic encephalitis.^{5,14} Our case also demonstrated perivascular lymphocytes, with the additional presence of neutrophils. There are reports documenting hemorrhagic white matter lesions with surrounding axonal injury and macrophages, associated with a perivascular acute disseminated encephalomyelitis appearance.¹⁵ These features were found in our case; however, acute disseminated encephalomyelitis was not considered as a differential diagnosis due to the primary documented large-vessel stroke. Another case study reported a florid leukocytoclastic reaction associated with infarcted tissue. This occurred together with lymphohistiocytic meningeal inflammation, although vasculitis distant from the infarct was not identified.⁴ Our case also showed a marked neutrophilic response to the infarct, together with distant vasculitis and intravascular thrombi, most prominent in the brainstem.

Acute infarcts in the brains of COVID-19 patients may be ischemic or hemorrhagic, and infarction may occur secondary to venous sinus thrombosis.⁶ They are histopathologically described as being small, patchy, peripheral, and deep neocortical ischemic lesions with microthrombi and focal parenchymal T-lymphocyte infiltrates.¹⁶ Associated hemorrhages suggest vascular damage and reperfusion injury.^{3,16} Macroscopically, they may be large, occurring in multiple arterial territories.^{4,6} Our case involved both MCA and ACA territories, with the occlusive thrombus identified on angiogram as being in the M1 branch of the left MCA. Partial reperfusion occurred following thrombectomy, contributing to hemorrhagic transformation.

CONCLUSIONS

There is considerable complexity in detangling primary neurological pathology from that due to general hypoxia or iatrogenic intervention, and several mechanisms may be at play in an individual patient. In addition to the large-vessel arterial territory infarct, the finding of multiple microinfarcts bilaterally throughout the white matter and cortex in our case may suggest that these lesions were related to separate microthrombi, which were also identified distant from the macroscopically involved region. The presence of a mixed cell vasculitis and meningeal inflammation in several locations raises the possibility that this process was not secondary to the MCA stroke, but rather an independent effect of SARS-CoV-2.

In terms of the medicolegal investigation of this case, consideration was given to postprocedure reperfusion injury with hemorrhagic transformation of the ischemic area and the possible contribution of anticoagulant therapy to this picture. Nonetheless, forensic pathology deemed this death to be “natural,”

with the cause of death given as “cerebrovascular accident associated with COVID-19.”

This case report offers a comprehensive description of a COVID-19–associated stroke in a young patient, with clinical, radiological, and histopathological correlation.

ACKNOWLEDGMENTS

The authors thank Mr Jurgen Geitner, senior technical officer, Pathology Learning Centre, University of Cape Town, for the expert assistance with the images used in this article; and Morton and Partners Radiologists, Melomed Gatesville Private Hospital, Cape Town, for the CT scan images and interpretation.

REFERENCES

- South K, McCulloch L, McColl BW, et al. Preceding infection and risk of stroke: an old concept revived by the COVID-19 pandemic. *Int J Stroke*. 2020;15:722–732.
- Jaunmuktane Z, Mahadeva U, Green A, et al. Microvascular injury and hypoxic damage: emerging neuropathological signatures in COVID-19. *Acta Neuropathol*. 2020;140:397–400.
- Otero JJ. Neuropathologists play a key role in establishing the extent of COVID-19 in human patients. *Free Neuropathology*. 2020; Bd. 1 (2020). Available at: <https://search.datacite.org/works/10.17879/freeneuropathology-2020-2736>. doi:10.17879/freeneuropathology-2020-2736. Accessed August 11, 2020.
- Adám Dénes, Allan S, Tibor Hortobágyi, et al. Studies on inflammation and stroke provide clues to pathomechanism of central nervous system involvement in COVID-19. *freeneuropathology*. 2020; 1(0). Available at: <https://www.uni-muenster.de/Ejournals/index.php/fnp/article/view/2818>. doi:10.17879/freeneuropathology-2020-2818. Accessed August 11, 2020.
- Montalvan V, Lee J, Bueso T, et al. Neurological manifestations of COVID-19 and other coronavirus infections: a systematic review. *Clin Neurol Neurosurg*. 2020;194:105921.
- Wu Y, Xu X, Chen Z, et al. Nervous system involvement after infection with COVID-19 and other coronaviruses. *Brain Behav Immun*. 2020;87:18–22.
- Beyroufi R, Adams ME, Benjamin L, et al. Characteristics of ischaemic stroke associated with COVID-19. *J Neurol Neurosurg Psychiatry*. 2020;91(8):889–891.
- Li Y, Li M, Wang M, et al. Acute cerebrovascular disease following COVID-19: a single center, retrospective, observational study. *Stroke Vasc Neurol*. 2020;5(3):279–284.
- Oxley TJ, Mocco J, Majidi S, et al. Large-vessel stroke as a presenting feature of COVID-19 in the young. *N Engl J Med*. 2020;382(20):e60.
- Umapathi T, Kor AC, Venketasubramanian N, et al. Large artery ischaemic stroke in severe acute respiratory syndrome (SARS). *J Neurol*. 2004; 251(10):1227–1231.
- Koralnik IJ, Tyler KL. COVID-19: a global threat to the nervous system. *Ann Neurol*. 2020;88(1):1–11.
- Kannemeier C, Shibamiya A, Nakazawa F, et al. Extracellular RNA constitutes a natural procoagulant cofactor in blood coagulation. *Proc Natl Acad Sci U S A*. 2007;104(15):6388–6393.
- Solomon IH, Normandin E, Bhattacharyya S, et al. Neuropathological features of COVID-19. *N Engl J Med*. 2020;383(10):989–992.
- von Weyhem CH, Kaufmann I, Neff F, et al. Early evidence of pronounced brain involvement in fatal COVID-19 outcomes. *Lancet*. 2020;395(10241):e109.
- Reichard RR, Kashani KB, Boire NA, et al. Neuropathology of COVID-19: a spectrum of vascular and acute disseminated encephalomyelitis (ADEM)-like pathology. *Acta Neuropathol*. 2020;140(1):1–6.
- Bryce C, Grimes Z, Pujadas E, et al. Pathophysiology of SARS-CoV-2: targeting of endothelial cells renders a complex disease with thrombotic microangiopathy and aberrant immune response. The Mount Sinai COVID-19 autopsy experience. *medRxiv*. 2020; 2020.05.18.20099960. Available at: <http://medrxiv.org/content/early/2020/05/22/2020.05.18.20099960>. abstract. doi:10.1101/2020.05.18.20099960. Accessed August 11, 2020.